Mechanical and acoustic properties of ceramsite sound absorbing boards with gradient structure

Zhuo Tang (zhuo.tang@csu.edu.cn)
Central South University
Kai Yang
Central South University
Guangcheng Long
Central South University
Xiaoyan Pan
China Railway Design Corporation
Weiqing Su
China Railway Design Corporation
Youjun Xie
Central South University

Research Article

Keywords: Ceramsite sound absorbing boards, Gradient structure, Mechanical properties, Acoustic properties, Physical structure model

Posted Date: April 26th, 2022

DOI: https://doi.org/10.21203/rs.3.rs-1586875/v1

Mechanical and acoustic properties of ceramsite sound absorbing boards with gradient structure

Kai Yang[1], Guangcheng Long[1], Zhuo Tang[1*], Xiaoyan Pan[2], Weiqing Su[2], Youjun Xie[1]

[1] School of Civil Engineering, Central South University, Changsha 410075, Hunan, China
[2] China Railway Design Corporation, Tianjin 300308, China

*Corresponding author: Zhuo Tang, E-mail address: zhuo.tang@csu.edu.cn

Abstract

In this work, ceramsite was utilized to fabricate the sound-absorbing boards, in which two types of structure were considered, specifically, single-layer board with homogenous structure and double-layer board with gradient structure. The mechanical and acoustic properties of these prepared ceramsite sound absorbing boards were studied, including the bulk density, compressive strength, flexural strength, softening coefficient, sound absorption coefficient and sound reduction index. The results show that the double-layer board with the appropriate mix proportion exhibited the almost identical bulk density and mechanical strength to the single-layer board. All ceramsite sound absorbing boards had compressive and flexural strengths of more than 3MPa and 1MPa, respectively, and also demonstrated good water resistance. In terms of sound absorption and sound insulation properties, the overall performance of the double-layer board with reasonable gradient structure was better than that of the single-layer board. In addition, the physical structure models of ceramsite sound absorbing boards were established to illustrate the variation of mechanical properties and explore the mechanism of sound absorption and insulation in the material.

Keywords Ceramsite sound absorbing boards; Gradient structure; Mechanical properties; Acoustic properties; Physical structure model

1 Introduction

With the rapid development of modern industry and transportation industry, noise pollution is becoming more and more serious. It has been reported that noise pollution has escalated into a contemporary worldwide problem, which is listed as one of the four major global pollutions, alongside water pollution, air pollution, and solid waste pollution [1]. The relevant surveys have suggested that the residents usually exposed to noise pollution could suffer from hearing loss, and under severe cases, their incidence rate of heart attack would be increased greatly [1,2]. Especially in the human settlements adjacent to highways, urban viaducts, and high-speed railways, the impact of noise has emerged as an increasingly significant issue that justifies considerable effort [2]. Therefore, the urgency to take effective measures of sound absorption and insulation to mitigate noise propagation and protect individuals from overexposure is evident.

Porous sound-absorbing materials have been widely used in noise reduction due to their porous porosity structure, particularly in sound absorption. The major function of porous structures was to provide superior sound absorption performance by the friction behavior of the wall of the pores and the viscosity effect of the air in the pores [3,4]. Generally, porous sound-absorbing materials can be classified into organic fibrous materials, inorganic fibrous materials, foam sound absorption materials, metal sound absorption materials, and cement-based sound absorption materials [5,6]. The fibrous and foam materials had the main disadvantage of poor strength and durability, and the cost of metal sound absorption materials was too expensive nowadays. Thus, several academics [7,8,9,10] have investigated cement-based ceramsite sound absorbing materials, attributing their good sound-absorbing capabilities, adjustable mechanical and durability properties, as well as their considerable economic benefits and environmental sustainability. From the characteristics of raw materials, ceramsite is a type of artificial and environmentally friendly aggregate made of clay or shale and manufactured by high-

51 temperature calcination. It is featured with a porous internal structure with a honeycomb shape inside
52 [9,10]. As a result, ceramsite is a light and porous raw material that is very suitable for sound
53 absorption. On the other hand, cement-based ceramsite sound absorbing material is formed by
54 wrapping and bonding ceramsite particles with cement paste. It means that in addition to the pores that
55 existed in the ceramsite itself, numerous voids are formed by the mutual accumulation of ceramsite
56 particles [10], thereby the ceramsite porous materials exhibit good sound absorption performance.
57 Existing studies by Luan et al. [7] and Wu et al. [10] have reported that the average sound absorption
58 coefficient (arithmetic mean of sound absorption coefficients of six frequencies, i.e., 125 Hz, 250 Hz,
59 500 Hz, 1000 Hz, 2000 Hz, and 4000 Hz) of the ceramsite porous material was greater than 0.5.
60 Besides, ceramsite sound absorbing material belongs to cement-based material, which can achieve
61 various properties such as strength and durability.

62 Many existing studies reveal that ceramsite sound absorbing material has good sound-absorbing
63 performance at high frequency, but its sound-absorbing coefficients at the low and medium frequencies
64 usually lead to unsatisfactory results [11,13,21]. Currently, scholars have adopted some measures to
65 improve the sound absorption coefficient at low and medium frequencies, such as increasing the
66 thickness of the material and reserving an air cavity with a certain thickness behind the material
67 [12,21,23]. However, increasing the thickness of the material would increase the bulk density and cost
68 of the material. Also, although the method of reserving air cavity behind the material improves sound
69 absorption performance at low and medium frequencies, ceramsite sound absorbing materials still have
70 a narrow sound absorption band [12,13,14,17]. What's more, for field applications, such as acoustic
71 barriers for traffic noise mitigation, in addition to meeting the sound insulation requirements, the
72 physical and mechanical properties of ceramsite sound absorbing materials should also be investigated

to ensure that the materials have sufficient strength and durability to resist the influence of environmental agents [24]. Therefore, it is necessary to conduct a relevant study on the mechanical and acoustic properties of ceramsite sound absorbing boards with gradient structure to give full play to their advantages and broaden their field application in sound absorption and insulation.

Given the above, single-layer and double-layer ceramsite sound absorbing boards were designed and manufactured in this work. The basic physical-mechanical properties and acoustic properties of these developed boards were studied. Based on the test findings, the effect of gradient structure on physical-mechanical properties and acoustic properties were investigated. At last, the corresponding mechanism was discussed by establishing the physical structure model of material. Overall, this research aimed to provide theoretical reference and technical support for preparing gradient-structured ceramsite sound absorbing materials used in field applications.

2 Experimental programs

2.1 Design and preparation of ceramsite sound absorbing boards

Two types of commercial ceramsite were used as the aggregates, including coarse ceramsite and fine ceramsite. The particle ranges of coarse and fine ceramsite were 0-5 mm and 0-3 mm, respectively. The particle size distributions of coarse and fine ceramsite are shown in Fig. 1. The cement paste was used as the binder, which was mainly composed of P·O 42.5 cement and water. In this study, three kinds of mix proportions (i.e., ①~③) were designed for the ceramsite sound absorbing material in consideration of particle gradation of ceramsite and content of cement paste. The details of the mix proportions are presented in Table 1. The mix ① adopted all coarse ceramsite as the aggregates, and the mix ② used half of each coarse and fine ceramsite as the aggregates, while the mix ③ adopted higher content of cement paste compared to mix ②.

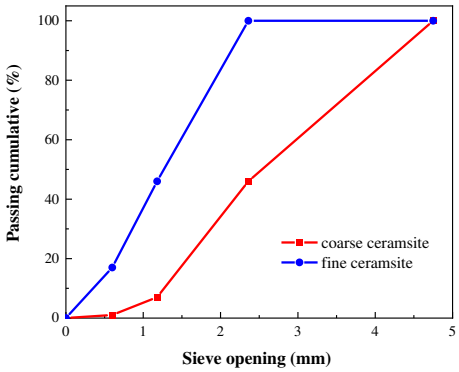

Fig. 1 Particle size distributions of coarse and fine ceramsite

Table 1 Mix proportions of ceramsite sound absorbing materials (kg/m^3)

Mix	Coarse ceramsite	Fine ceramsite	Cement paste
①	710	0	242
②	355	355	242
③	355	355	805

Based on the above mix proportions, three types of ceramsite sound absorbing boards were designed. Specifically, specimen A was a single-layer board prepared by the mix ①, while specimens B and C were double-layer boards prepared by mix ① and mix ② or ③. The length and width of sound-absorbing boards were about 975 mm and 495 mm, respectively. The details of the design schemes are presented in Table 2. The ceramsite sound absorbing boards were manufactured by industrial production technology. The raw materials were mixed and stirred according to the corresponding mix proportion, and then, the ceramsite sound absorbing boards were formed by vibratory compaction. The pressure during the vibratory was around 15kN, and the vibratory compaction was maintained for 2-4s. Fig. 2(a) and (b) show the vibratory compaction equipment and the formed sound-absorbing boards, respectively.

Table 2 Design schemes of ceramsite sound absorbing boards

Specimens	The thickness of layer X	The thickness of layer Y	Total thickness
A（single-layer）	50-mm (①)	0-mm	50-mm
B（double-layer）	35-mm (①)	15-mm (②)	50-mm
C（double-layer）	35-mm (①)	15-mm (③)	50-mm

(a) Vibratory compaction equipment

(b) Formed sound absorbing boards

Fig. 2 Vibratory compaction equipment and formed sound-absorbing boards

The formed ceramsite sound absorbing boards were covered with plastic films for preventing the evaporation of free water in mixtures, and then, were stored in a closed room at ambient temperature for curing. After curing for 28 days, experimental tests were carried out to evaluate the performance of the specimen according to the following test methods.

2.2 Test methods

2.2.1 Physical and mechanical properties

The physical and mechanical properties of the specimen, i.e., bulk density, compressive strength, flexural strength, and softening coefficient, were tested as per Chinese standards of [15] and [16]. Three plate specimens with a dimension of 100×100×50 mm were used for the measurement of the bulk density of each group; Three plate specimens with a size of 100×100×50 mm were tested for the compressive strength of each group, and the compressive surface of specimens was 100×100 mm; One plate specimen with a size of 250×250×50 mm was tested for the flexural strength of each group. The flexural strength of the specimen was tested by three-point bending test as per the Chinese standard of [15], in which the force (F) was loaded in the two directions on the midspan of the specimen successively. The schematic diagram of the flexural strength test is shown in Fig. 3. The flexural strength in one direction on the midspan of the specimen was calculated via Eq. (1).

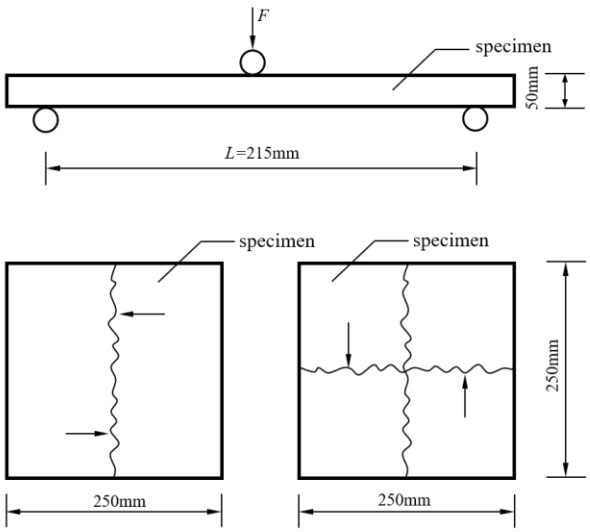

Fig.3 Schematic diagram of flexural strength test

$$f_t = \frac{3FL}{2be^2} \quad (1)$$

where f_t is the flexural strength (MPa); F is the peak load (N); L is the span (mm); b and e are respectively the width and thickness of the section subjected to flexure (mm).

The softening coefficient was used to characterize the water resistance of the specimen, it was the ratio of the compressive strength of the specimen in the water-saturated state to that under the dry state. The water-saturated state was achieved by immersing the specimen in water at 20±2℃ for 3d. And the test method was following the above-mentioned compressive strength test. It should be noted that all the above specimens for physical and mechanical properties testing were cored from the corresponding sound-absorbing boards, and the average of the multiple test results was taken as the final result.

2.2.2 Acoustic properties

In this study, the sound absorption coefficients and the sound reduction indexes at the frequencies of 125-4000 Hz were tested to evaluate the acoustic properties of the prepared ceramsite sound absorbing boards. The sound absorption coefficients were measured in a reverberation room (as shown in Fig. 4). 20 pieces of ceramsite sound absorbing boards (the total area of ceramsite sound absorbing boards was about 10 square meters) were laid in the room for sound absorption measurements. In the

reverberation room, the irregular incidence sound absorption coefficients of sound absorbing materials were measured and the acoustic field was diffuse, which was closer to the actual service conditions. Thus, the sound absorption coefficients obtained by the reverberation room could accurately reflect the sound absorption performance of the materials in service. The sound reduction indexes were measured in a sound insulation test room (as shown in Fig. 5). The sound insulation test room consisted of two adjacent reverberation rooms, i.e., the sound source room and the sound reception room. Between the two rooms with the test hole for the installation of ceramsite sound absorbing boards.

Fig.4 Reverberation room

Fig.5 Sound insulation test room

3 Results and analyses

3.1 Physical and mechanical properties

Fig. 6 shows the physical and mechanical properties of ceramsite sound absorbing specimens. It can be observed from Fig. 6(a) that the bulk densities of all the specimens were lower than 1000 kg/m^3. As an example, the bulk density of specimen B was 860.8 kg/m^3, which was about 1/3 times the density of concrete (around 2400 kg/m^3). Also, the bulk density of double-layer specimens B and C was greater than that of the single-layer specimen A. Specifically, the bulk density of specimen B was increased by 1.2%, and the bulk density of specimen C was increased by 17.3%, compared with specimen A. This was attributable to the more compact accumulation of ceramsite in layer Y of specimens B and C due to the mixing of coarse and fine ceramsite, as well as the fact that layer Y of specimen C had large content of cement paste, which had a higher density than ceramsite.

As demonstrated in Fig. 6(b), the compressive strengths of all specimens were greater than 3MPa. The compressive strength of double-layer specimen B was marginally lower than that of single-layer specimen A, while the compressive strengths of specimens A and B was respectively decreased by 7.8% and 10.7% compared with specimen C. As shown in Fig. 6(c), the flexural strengths of all specimens were greater than 1MPa. Comparatively, the flexural strength of double-layer specimen C was the highest, which was almost twice that of specimens A and B. This was because that the flexural strength was mainly determined by the tensile strength of bottom portion, and the layer Y of specimen C had higher tensile carrying capacity attributed to the high-content cement paste. Besides, the mechanical strengths of specimens A and B did not differ significantly, with the variation less than 10%.

It can also be found from Fig. 6(d) that the softening coefficients of specimens A, B, and C were greater than 0.80, indicating that both single-layer and double-layer specimens exhibited good water resistance. Compared with single-layer specimen A, the softening coefficient of specimen B was increased by 5.7% and reached 0.92, while the softening coefficient of specimen C was decreased by 4.8%.

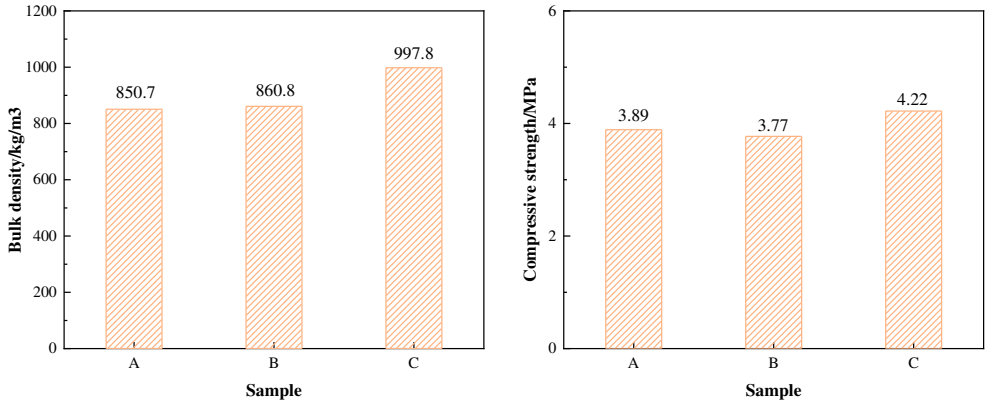

(a) Bulk density (b) Compressive strength

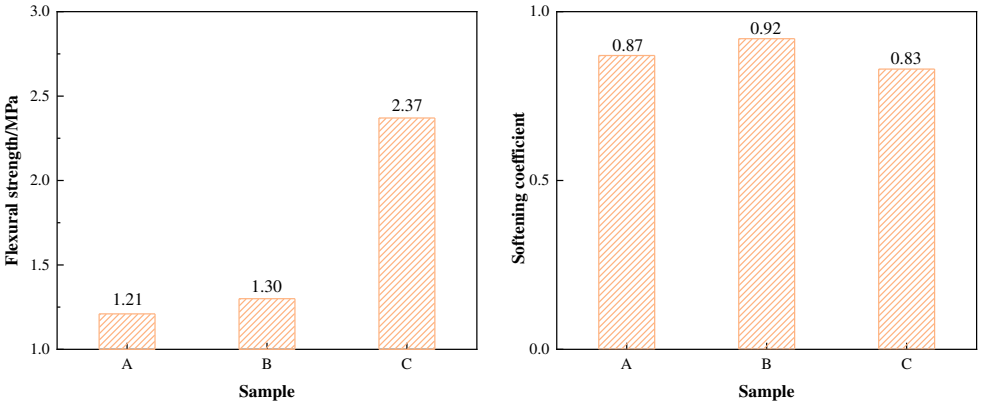

(c) Flexural strength (d) Softening coefficient

Fig.6 Physical and mechanical properties of ceramsite sound absorbing specimens

3.2 Acoustic properties

3.2.1 Sound absorption properties

Fig. 7 shows the sound absorption coefficients at 125-4000 Hz of specimens A, B and C. The experimental results show that the sound absorption coefficients at 125-2000 Hz of specimen B were higher than that of specimen A. In particular, the sound absorption coefficients at 125 Hz, 250 Hz, 500Hz, 1000 Hz and 2000 Hz of specimen B were respectively increased by 14.3%, 7.7%, 12.5%, 7.4%, 24.6% compared with specimen A. This indicates that employing proper gradient structure could improve the sound absorption performance at 125-2000 Hz. Moreover, the sound absorption coefficients at 125-1000 Hz of specimen C were lower than those of specimen A, while the absorption coefficients at 2000 Hz of specimen C were higher than those of specimen A. It suggests that the high compactness adopted in the layer Y of specimen C was not conducive to enhancing the sound absorption performance at low and medium frequencies of the specimen, but could improve the sound absorption property at higher frequency of 2000 Hz. It is worth noting that specimen A exhibited the highest sound absorption coefficient at 4000 Hz, which was followed by specimen B and specimen C. In addition, the comparison between the double-layer specimens B and C shows that the sound absorption coefficients at 125-1000 Hz and 4000 Hz of specimen B were all higher than those of specimen C; while at the frequency of 2000 Hz, the sound absorption coefficient of specimen B was

lower than that of specimen C.

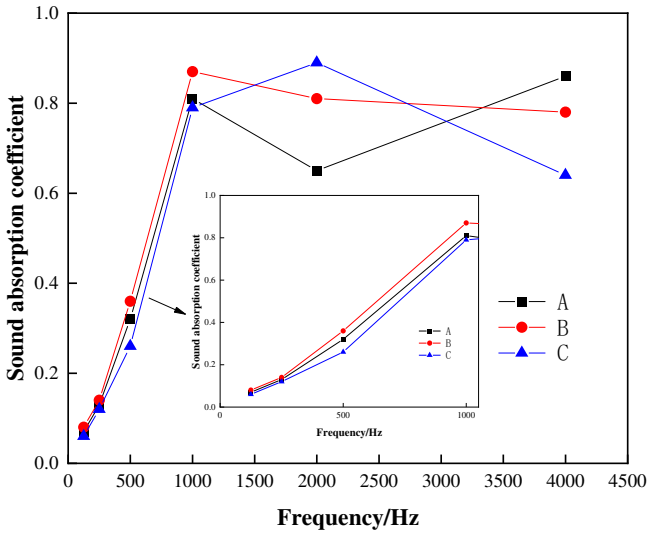

Fig. 7 Sound absorption coefficients at 125-4000 Hz of specimens A, B and C

The noise reduction coefficient (*NRC*) and the average sound absorption coefficient ($\overline{\alpha}$) were employed to evaluate the overall sound absorption performance of the specimens, as stipulated in the Chinese standard of [18]. Thereinto, *NRC* and $\overline{\alpha}$ were calculated via Eqs. (2) and (3), respectively.

$$NRC=\frac{\alpha_{250}+\alpha_{500}+\alpha_{1000}+\alpha_{2000}}{4} \quad (2)$$

$$\overline{\alpha}=\frac{\alpha_{125}+\alpha_{250}+\alpha_{500}+\alpha_{1000}+\alpha_{2000}+\alpha_{4000}}{6} \quad (3)$$

Where α_{125}, α_{250}, α_{500}, α_{1000}, α_{2000} and α_{4000} were the sound absorption coefficient at 125 Hz, 250 Hz, 500 Hz, 1000 Hz, 2000 Hz, and 4000 Hz, respectively.

Table 3 *NRC* and $\overline{\alpha}$ of specimens A, B and C

Specimens	*NRC*	$\overline{\alpha}$
A（single-layer）	0.48	0.48
B（double-layer）	0.55	0.51
C（double-layer）	0.52	0.46

Table 3 shows the *NRC* and $\overline{\alpha}$ of specimens A, B and C. It can be found that specimen B had the highest *NRC* and $\overline{\alpha}$, indicating that the sound absorption property of double-layer specimen B with reasonable gradient structure was the best. It is worth noting that the *NRC* of specimen C was higher than that of specimen A, while the $\overline{\alpha}$ of specimen C was lower than that of specimen A. This was

reasonable as that specimen A exhibited a higher sound absorption coefficient at 4000 Hz compared with specimen C, resulting in a higher average sound absorption coefficient ($\overline{\alpha}$) for specimen A. In other words, compared to specimen A, specimen C exhibited better sound absorption performance at 250-2000 Hz, but worse sound absorption property at 125-4000 Hz.

3.2.2 Sound insulation properties

Fig. 8 shows the sound reduction indexes at 125-4000 Hz of specimens A, B, and C. It can be observed that the sound reduction indexes at 125-4000 Hz of specimen C was the highest, with the sound reduction index ranging from 14-20 dB. The subsequent were specimen B and specimen A, which had the sound reduction index ranging from 11-15 dB and 4-9 dB, respectively.

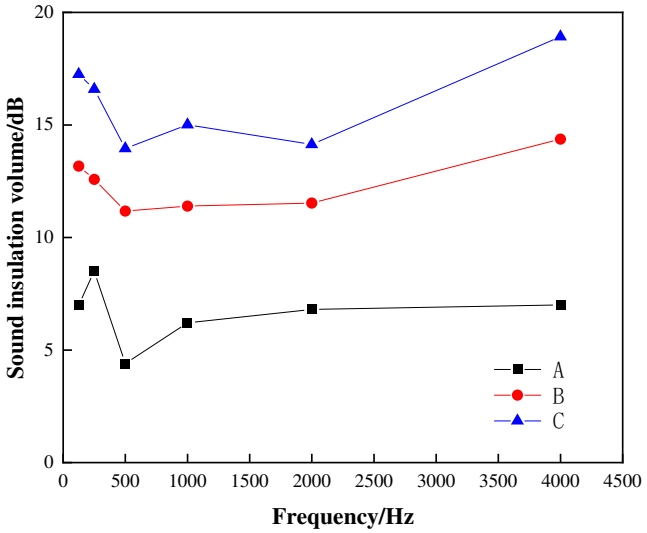

Fig. 8 Sound reduction indexes at 125-4000 Hz of specimens A, B, and C.

Table 4 gives the average sound reduction index ($\overline{R}$) of specimens A, B, and C, which was calculated via Eq. (4).

$$\overline{R} = \frac{R_{125} + R_{250} + R_{500} + R_{1000} + R_{2000} + R_{4000}}{6} \quad (4)$$

Where R_{125} , R_{250} , R_{500} , R_{1000} , R_{2000} and R_{4000} were the sound reduction index at 125 Hz, 250 Hz, 500 Hz, 1000 Hz, 2000 Hz, and 4000 Hz, respectively.

Table 4 The average sound reduction index ($\overline{R}$) of specimens A, B, and C

Specimens	$\overline{R}$ / dB
A（single-layer）	6.58
B（double-layer）	11.97
C（double-layer）	15.39

It can be found from Table 4 that the $\overline{R}$ of double-layer specimen was higher than that of single-layer specimen, specifically, the $\overline{R}$ of specimens B and C was increased by 81.9% and 133.9%, respectively, compared with the specimen A. This indicates that the sound insulation properties at 125-4000 Hz of double-layer specimens B and C were significantly enhanced by introducing gradient structure compared with single-layer specimen A. Moreover, the $\overline{R}$ of double-layer specimen C was higher than that of double-layer specimen B due to the high-content cement paste adopted in the layer Y of specimen C.

From the above results of sound absorption coefficient and sound reduction index, it can be concluded that specimen B with appropriate gradient structure not only improved the sound absorption properties but also enhanced the sound insulation performance compared with the single-layer specimen A. It suggests that using proper gradient structure had a positive effect on improving the acoustic performance, i.e., sound absorption properties and sound insulation properties, of the ceramsite sound absorbing board. In addition, the average absorption coefficient of specimen C was decreased compared with the specimen B due to the high-content cement paste in the layer Y, which obstructed the entry and consumption of sound waves to some extent. However, it is worth mentioning that the sound insulation property of specimen C was the best among the three groups of specimens A, B and C due to the dense structure of layer Y.

4 Discussions

4.1 Physical structure model

A good understanding of the relationship between compositions, structures, and properties of ceramsite porous boards with gradient structure was important, the corresponding physical structure

model was established according to the cross-section view of specimens A, B and C (as shown in Fig. 9). The physical structure models of specimens A, B, and C were shown in Figs. 10(a), (b) and (c), respectively. The established model was based on the considerations of gradient structure and the assumption that ceramsite particles with different sizes were regular spheres. The accumulation state of ceramsites and the process of absorption, reflection, and transmission of the acoustic wave in ceramsite porous materials were shown by the model. Thereinto, incident sound energy, reflected sound energy, absorbed sound energy, consumed heat energy, and transmitted sound energy was expressed as E_{in}, E_{re}, E_{ab}, E_{heat}, and E_{tr}, respectively.

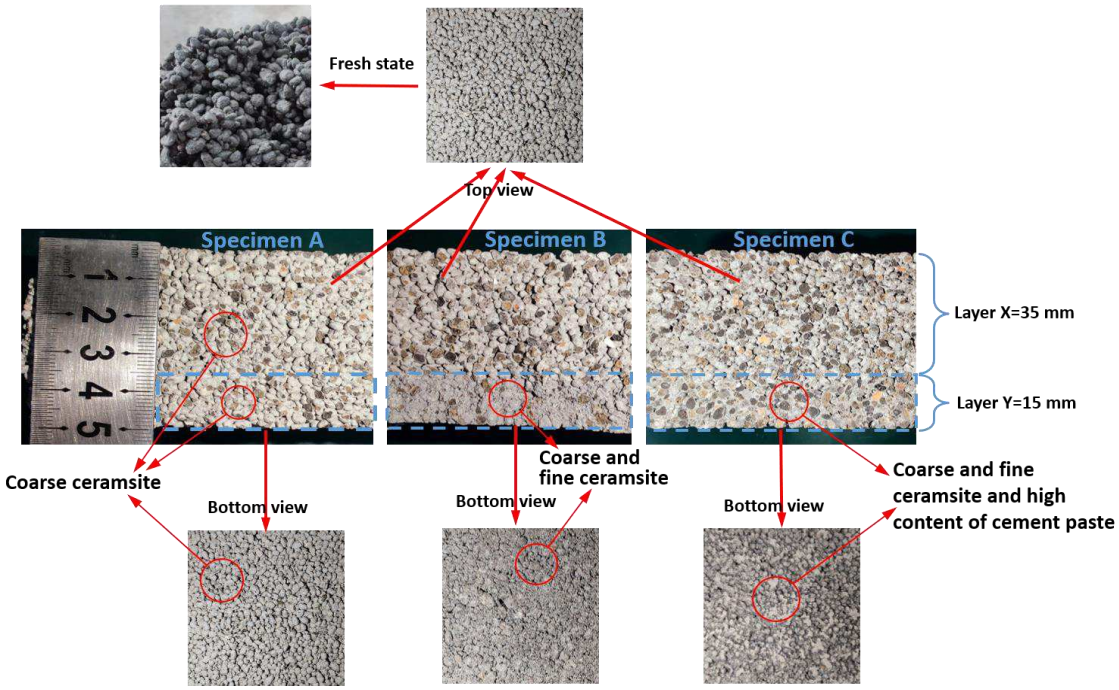

Fig. 9 Cross-section view of specimens A, B and C

For mechanical properties, it can be seen from Fig. 10(a) that the ceramsite sound-absorbing specimen was composed of ceramsite coated with a layer of cement paste, and there was a weak area between ceramsite and cement paste, i.e., interface transition zone (ITZ) [19]. This suggests that the strength of ceramsite porous material was governed by the strength of aggregate phase (the strength of

ceramsite itself), the strength of cement paste, and the bond strength between ceramsite and cement paste, which was consistent with the opinion of Ref [10]. When the number and gradation of ceramsite phase remained constant, the bond strength between ceramsite and cement paste was dependent on the content of cement paste on the surface of ceramsite. In comparison with the layer Y of specimen B, there were more adhesive sites between adjacent ceramsites in the layer Y of specimen C due to the higher content of cement paste adopted. Thus, the strength of layer Y of specimen C was higher, resulting in the overall compressive and flexural strengths of specimen C being higher than those of specimen B. Moreover, the denser structure from the mixture of coarse and fine ceramsite had a positive effect on the specimen's strength. At the same time, the total surface area of ceramsite was increased through the mixing of coarse and fine ceramsite, thus the content of cement paste on the surface of ceramsite was reduced when the total content of cement paste remained constant, resulting in a reduction in the specimen's strength. As a result, the contribution of the above positive and negative effects led to little variation in the strength of layer Y of specimen B compared to specimen A, as well as in the overall compressive and flexural strengths between specimens A and B.

For sound absorption properties, it can be observed from Fig. 10(a) that the incident sound energy entered the interior of single-layer specimen A when the normal incident acoustic wave was propagated to its surface. There were two main ways to absorb sound energy by the material of layer X. One was that in the process of acoustic wave propagation inside layer X, the acoustic wave vibrated the air of micropores or voids in the materials. The other was that acoustic waves rubbed with the pore wall of ceramsite. The above two main ways led to the sound energy being consumed according to the viscosity resistance of air and the friction effect of the wall of the pores [6,20]. Subsequently, the transmitted sound energy was formed when the acoustic wave passed through the layer X.

292 Fig. 10(b) shows the physical structure model of the double-layer specimen B. Unlike specimen A
293 which had only one size of pores, specimen B included two sizes of pores due to the two layers with
294 different mixture design. Thus, when the acoustic wave was propagated to the interface between layer
295 X and layer Y, in addition to part of the acoustic wave entering the layer Y, the other part of the acoustic
296 wave was reflected into layer X for another round of consumption. This was attributed that when the
297 sound waves entered the interface of different media, the reflection phenomenon of sound waves would
298 occur due to the different sound resistivity of the media [20,22]. So the double-layer specimen B had
299 two different media (layer X and layer Y), leading to multiple reflection and propagation of sound
300 waves [22,25,26], thus considerably consuming the sound energy. Therefore, specimen B with proper
301 gradient structure exhibited higher sound absorption coefficients at basically all frequencies than those
302 of specimen A. As a result, the double-layer specimen B had a higher average sound absorption
303 coefficient of 125-4000 Hz compared with the single-layer specimen A.
304 Fig.10(c) shows the physical structure model of the double-layer specimen C. It can be observed
305 that layer Y of specimen C was denser compared with specimen B because the internal void was filled
306 with high-content cement paste. When the incident sound energy reached the interface of layers X and
307 Y, most of the sound wave was reflected into layer X, and only a small part of the sound energy was
308 consumed due to the lack of pores or voids in layer Y of the specimen C. As a result, specimen C
309 depended primarily on the sound-absorbing material of layer X to achieve sound absorption, resulting
310 in the lowest average sound absorption coefficient among the three groups of specimens A, B, and C.
311 Additionally, for sound insulation properties, specimen A was the single-layer board with a
312 homogenous structure prepared by coarse ceramsite, which meant the overall pore size of specimen A
313 was the largest among the three groups of specimens. Also, the layer Y of specimen B adopted a

mixture of coarse ceramsite and fine ceramsite, and the layer Y of specimen C added more cement paste to the mixture of coarse ceramsite and fine ceramsite. So the compactness of layer Y of specimen C was higher than that of specimen B. The sound insulation principle suggested that the denser the material (the smaller the pore size), the better the sound insulation property [27]. Therefore, the value of transmitted sound energy of specimen A (E_{tr1}) was the largest, which was followed by specimen B (E_{tr2}) and specimen C (E_{tr3}). This was consistent with the results of sound insulation properties in this research. It indicates that the sound insulation performance of the double-layer specimen was better than that of the single-layer specimen, and the sound reduction index was enhanced with the increase of the compactness of the layer Y in the double-layer specimen. In conclusion, an appropriate gradient structure adopted in ceramsite sound absorbing boards could play a good dual role in sound absorption and sound insulation.

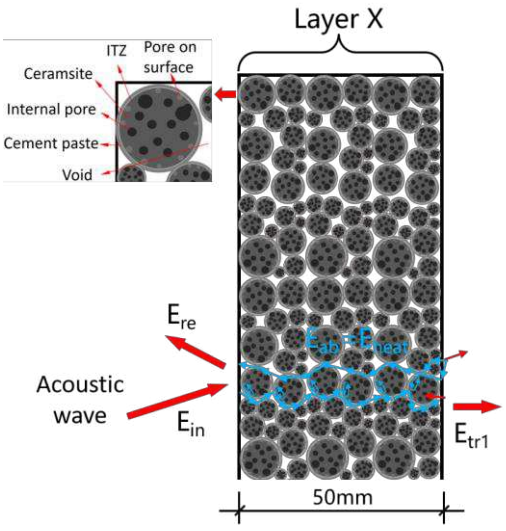

(a) Single-layer specimen A

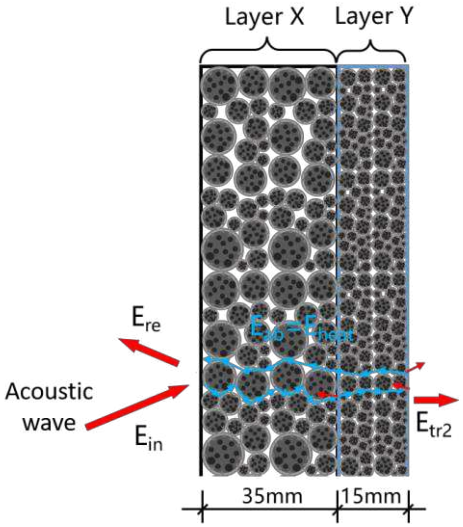

(b) Double-layer specimen B

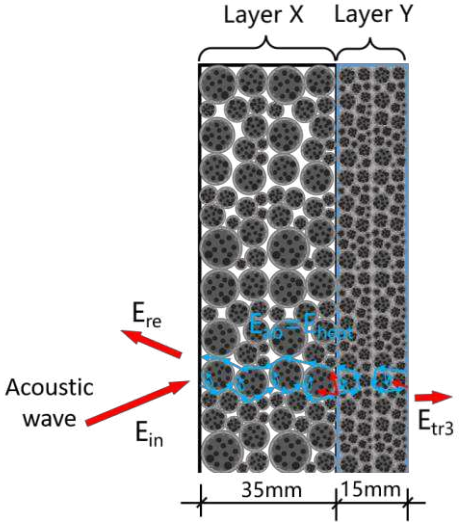

(c) Double-layer specimen C

Fig. 10 Physical structure model of ceramsite sound absorbing boards

5 Conclusions

To provide theoretical reference and technical support for preparing gradient-structured ceramsite sound absorbing boards used in field applications, single-layer and double-layer ceramsite sound absorbing boards were designed and manufactured. The mechanical and acoustic properties, including the bulk density, compressive strength, flexural strength, softening coefficient, sound absorption coefficients at 125-4000 Hz and sound reduction indexes at 125-4000 Hz, of these prepared ceramsite sound absorbing boards were studied. At last, the corresponding mechanism was discussed. Based on the results from this study, the following conclusions can be drawn:

1. The bulk density, compressive strength, and flexural strength of double-layer ceramsite sound absorbing board with suitable mix proportion design were almost identical to those of single-layer ceramsite sound absorbing board.

2. The compressive and flexural strengths of ceramsite sound absorbing boards were greater than 3MPa and 1MPa, respectively. All ceramsite sound absorbing boards in this work demonstrated good water resistance, with softening coefficients greater than 0.80. Such good strength and durability of ceramsite sound absorbing boards support their field application in future.

3. Introducing proper gradient structure could improve the sound absorption performance at low and medium frequencies of ceramsite sound absorbing boards. The double-layer board B with reasonable gradient structure exhibited better overall sound absorption properties and overall sound insulation performance at 125-4000 Hz compared with the single-layer board A.

4. The sound insulation properties at 125-4000 Hz of double-layer specimens B and C adopted gradient structure were significantly enhanced compared with the single-layer specimen A. What's more, the compactness of layer Y in double-layer board could not be too high, otherwise it would reduce the sound absorption property at 125-1000 Hz of ceramsite sound absorbing board.

5. The physical structure model successfully illustrated the process of absorption, reflection, and transmission of the acoustic wave in the material and explained the variation of mechanical and acoustic properties of ceramsite sound absorbing board.

Acknowledgments

The authors greatly acknowledge the financial support received from the science and technology development project of China Railway Design Corporation (Grant No.2021A240904), the Yunnan Provincial Department of Science and Technology Planning Project (Grant No.202004AR040022), and

the independent exploration project for postgraduates of Central South University (Grant No.2021zzts0783).

Author Contributions

Kai Yang: designed the research, processed the corresponding data, and wrote the first draft of the manuscript, Guangcheng Long and Zhuo Tang: acquired the funding, and revised and edited the manuscript, Xiaoyan Pan and Weiqing Su: provide test site and technical support, and proposed modification suggestions to the manuscript, Youjun Xie: helped perform the analysis of the manuscript with constructive discussions.

Funding

The science and technology development project of China Railway Design Corporation (Grant No.2021A240904), the Yunnan Provincial Department of Science and Technology Planning Project (Grant No.202004AR040022) and the independent exploration project for postgraduates of Central South University (Grant No.2021zzts0783).

Declarations

Conflict of interest The authors have no conflicts of interest to declare that are relevant to the content of this article.

References

1. Y. Tao, M. Ren, H. Zhang, et al., Recent progress in acoustic materials and noise control strategies-A review, Appl. Mater. Today **24**, 1-23 (2021). https://doi.org/10.1016/j.apmt.2021.101141

2. H. Kim, J. Hong, S. Pyo, Acoustic characteristics of sound absorbable high performance concrete, Appl. Acoust. **138**, 171-178 (2018). https://doi.org/10.1016/j.apacoust.2018.04.002

3. LM Peng, BQ Song, JF Wang, Wang D, Mechanic and acoustic properties of the sound-absorbing material made from natural fiber and polyester. Adv. Mater. Sci. Eng. **2015**, 274913 (2015). https://doi.org/10.1155/2015/274913

4. B.G Ma, Z.H Jin, Y. Su, et al., Utilization of hemihydrate phosphogypsum for the preparation of porous sound absorbing material, Constr. Build. Mater. **234**, 1-12 (2020). https://doi.org/10.1016/j.conbuildmat.2019.117346

5. J. Yoon, H. Kim, T. Koh, et al., Microstructural characteristics of sound absorbable porous cement-based materials by incorporating natural fibers and aluminum powder, Constr. Build. Mater. **243**, 1-11 (2020). https://doi.org/10.1016/j.conbuildmat.2020.118167

6. LD Gao, QX Fu, Y Si, et al. Porous materials for sound absorption. Compos. Commun. **10**, 25-35 (2018). https://doi.org/10.1016/j.coco.2018.05.001

7. H.X Luan, J. Wu, W.X Zhu, et al., Preparation and acoustic performance of recycled ceramsite concrete noise-absorbing plat, Journal of Central South University (Science and Technology) **51**(05), 1299-1308 (2020). https://doi.org/10.11817/j.issn.1672-7207.2020.05.014

8. W.F Li, X.Y Luo, X.L Jin, Effect of acoustic components on characteristics of ceramsite porous concrete, J. Build. Mater. **16**(01), 70-75 (2013), in Chinese. https://doi.org/10.3969/j.issn.1007-9629.2013.01.013

9. H.Q Wu, T. Zhang, R.J Pan, et al., Sintering-free preparation of porous ceramsite using low-temperature decomposing pore former and its sound-absorbing performance, Constr. Build. Mater. **171**, 367-376 (2018). https://doi.org/10.1016/j.conbuildmat.2018.03.152

10. H.Q Wu, T. Zhang, Y.Y Chun, et al., Development of high performance cement-based sound absorbing haydite, Journal of Guangxi University (Nat Sci Ed) **43**(01), 86-94 (2018), in Chinese.

https://doi.org/10.13624/j.issn.1001-7445. 2018. 0086

11. X.W Liu, X.W Ma, C.L Yu, et al., Sound absorption of porous materials perforated with holes having gradually varying radii, Aerosp. Sci. Technol. **120**, 1-16 (2022). https://doi.org/10.1016/j.ast.2021.107229

12. X.T Wang, L.F Ma, Y.S Wang, et al., Design of multilayer sound-absorbing composites with excellent sound absorption properties at medium and low frequency via constructing variable section cavities, Compos. Struct. **266**, 1-8 (2021). https://doi.org/10.1016/j.compstruct.2021.113798

13. C.C Zhang, J.X Gong, H.Q Li, et al., Fiber-based flexible composite with dual-gradient structure for sound insulation, Compos. Part B-Eng. **198**, 1-7 (2020). https://doi.org/10.1016/j.compositesb.2020.108166

14. C. Boutin, Acoustics of porous media with inner resonators, J. Acoust. Soc. Am. **134**(6), 4717-4729 (2013). https://doi.org/10.1121/1.4824965

15. Chinese National standard, Test methods for building wallboard, GB/T 30100-2013, China, Beijing, 2013, in Chinese.

16. Chinese National standard, Light weight panels for partition wall used in buildings, GB/T 23451-2009, China, Beijing, 2009, in Chinese.

17. Sheng TT, Hung MK, Azma P, et al. Sound absorption performance of modified concrete: A review. J. Build. Eng. **30**, 1-10 (2020). https://doi.org/10.1016/j.jobe.2020.101219

18. TB/T 3122-2019, Chinese railway industry standard, Acoustic elements of railway sound barrier, 2019, in Chinese.

19. A. Sidorova, E. Vazquez-Ramonich, M. Barra-Bizinotto, et al., Study of the recycled aggregates nature's influence on the aggregate–cement paste interface and ITZ, Constr. Build. Mater. **68**, 677-

684 (2014). https://doi.org/10.1016/j.conbuildmat.2014.06.076

20. J.P Song, The discussion of porous material air cavity and low frequency sound absorption effect, Noise and Vibration Control. **35**(S1), 312-315 (2015), in Chinese. https://doi.org/10.3969/j.issn.1006-1335.2016.01.079

21. B.S Kima, J.H Park, Double resonant porous structure backed by air cavity for low frequency sound absorption improvement, Compos. Struct. **183**, 545-549 (2018). https://doi.org/10.1016/j.compstruct.2017.06.027

22. J.L Zhu, J. Sun, H.P Tang, et al., Gradient-structural optimization of metal fiber porous materials for sound absorption, Powder Technol. **301**, 1235-1241 (2016). https://doi.org/10.1016/j.powtec.2016.08.006

23. XW Liu, CL Yu, FX Xin, Gradually perforated porous materials backed with Helmholtz resonant cavity for broadband low-frequency sound absorption. Compos. Struct. **263**, 113647 (2021). https://doi.org/10.1016/j.compstruct.2021.113647

24. M Pereira, J Carbajo, L Godinho, et al. Improving the sound absorption behaviour of porous concrete using embedded resonant structures, J. Build. Eng. **35**, 102015 (2021). https://doi.org/10.1016/j.jobe.2020.102015

25. X Chen, WT Ma, YD Hao, et al. Analysis and optimization design for sound absorption performance of gradient elastic porous materials. Journal of Vibration and Shock **40**(9) 270-277 (2021), in Chinese. https://doi.org/10.13465/j.cnki.jvs.2021.09.035

26. XY Gong, J Bustillo, L Blanc, et al. Acoustic properties study of porous materials with orthotropic symmetry and specific pore shapes-I. Analytical calculations. Journal of Sound and Vibration **516**, 116518 (2022). https://doi.org/10.1016/j.jsv.2021.116518

27. Z.X Kang, R.X Song, H.J Zhang, Study on sound insulation performance of double-layer perforated panel under normal incidence waves, Appl. Acoust. **174**, 1-10 (2021). https://doi.org/10.1016/j.apacoust.2020.107785